

ASSESSMENT OF UNCERTAINTY-BASED SCREENING VOLUMES FOR NASA ROBOTIC LEO AND GEO CONJUNCTION RISK ASSESSMENT

Steven Narvet,^{*} Ryan C. Frigm,^{*} and M.D. Hejduk[†]

Conjunction Assessment operations require screening assets against the space object catalog by placing a pre-determined spatial volume around each asset and predicting when another object will violate that volume. The selection of the screening volume used for each spacecraft is a trade-off between observing all conjunction events that may pose a potential risk to the primary spacecraft and the ability to analyze those predicted events. If the screening volumes are larger, then more conjunctions can be observed and therefore the probability of a missed detection of a high risk conjunction event is small; however, the amount of data which needs to be analyzed increases. This paper characterizes the sensitivity of screening volume size to capturing typical orbit uncertainties and the expected number of conjunction events observed. These sensitivities are quantified in the form of a trade space that allows for selection of appropriate screening volumes to fit the desired concept of operations, system limitations, and tolerable analyst workloads. This analysis will specifically highlight the screening volume determination and selection process for use in the NASA Conjunction Assessment Risk Analysis process but will also provide a general framework for other Owner / Operators faced with similar decisions.

INTRODUCTION

Since the first launch of man-made objects into space, there has always been interest in, and concern with, the collisions of objects in space. This interest has grown over the last decade from an academic curiosity to a set of policies and requirements levied on satellite operations. The space environment has become increasingly congested as new satellites are launched into orbit and have generated a significant debris environment due to on-orbit events such as explosions and collisions. In recent times, the number of objects in Earth orbit has been increasing markedly, and the threat of collision in space has now become of foremost concern to satellite Owner / Operators (O/O). This interest has peaked recently with the intentional destruction of the Fengyun 1-C spacecraft and the collision between the active Iridium-33 satellite and the defunct COSMOS-2251 satellite.

Spacecraft safety of flight has always been of principal concern to the National Aeronautics and Space Administration (NASA). In the late 1980s, the NASA Johnson Space Center (JSC)

^{*}Project Engineer, Mission Services Division, a.i. solutions Inc, 985 Space Center Drive, Colorado Springs, CO 80915.

[†]Adjunct Scientist, Mission Services Division, a.i. solutions Inc., 985 Space Center Drive, Colorado Springs, CO 80915.

began a program to receive close approach predictions to determine if a risk was posed to the space shuttle. In 2005, the NASA Goddard Space Flight Center (GSFC) took an active role in adopting and adapting this process for its unmanned, or robotic, assets. Both processes are still in existence today and have evolved to ensure safety of flight for all NASA missions. NASA / JSC still continues to perform routine conjunction assessment risk analysis for all manned NASA missions while NASA / GSFC performs this function for all robotic missions.

In both the human spaceflight and the robotic concept of operations, the process begins with generation of close approach predictions by the Joint Space Operations Center (JSpOC) at Vandenberg Air Force Base. This close approach prediction process at JSpOC consists of placing a keep-out volume (called a screening volume) around a primary object (the asset spacecraft) and “screening” it against the high accuracy catalog. For the robotic-mission process, which is the focus of the remainder of the paper, if any secondary object is predicted to violate the keep-out volume threshold, data on the close approach is sent to NASA / GSFC for further risk analysis. Selection of these keep-out volumes have large impacts on the overall safety of satellites due to conjunction risks as well as the workload at the JSpOC, NASA / GSFC, and NASA mission Owner / Operators (O/O). This analysis examines these screening volume trade-offs and the role they play in the trade space between mission safety and operational workload.

The analysis of the Low Earth Orbit (LEO) and Geosynchronous (GEO) Orbit regimes is categorized as defined in Table 1. Unless otherwise stated, conjunction data is always defined relative to the primary. For example, if a conjunction is identified against a primary that operates in the LEO #2 orbit regime, then all data related to that conjunction is compiled and used for statistical analysis of that (LEO #2) regime. This approach was chosen for several reasons. The first is that it is typical in conjunction analysis to define all data relative to the primary. The second reason, specifically for this analysis, is that a primary may observe conjunctions with objects outside a given regime (*i.e.* traverse through multiple regimes) and it is desired to collect data on any conjunctions from the perspective of the primary, regardless of the orbital regime of the other body.

Table 1: LEO and GEO Orbit Regime Definitions

| Orbital Regime | Definition |
|-----------------------|--------------------------------------------------------------------------------|
| LEO #1 | Perigee \leq 500 km & Eccentricity $<$ 0.25 |
| LEO #2 | 500 km $<$ Perigee \leq 750 km & Eccentricity $<$ 0.25 |
| LEO #3 | 750 km $<$ Perigee \leq 1200 km & Eccentricity $<$ 0.25 |
| LEO #4 | 1200 km $<$ Perigee \leq 2000 km & Eccentricity $<$ 0.25 |
| GEO | 1300 min $<$ Period $<$ 1800 min & Eccentricity $<$ 0.25 & Inclination $<$ 35° |

DETERMINING SENSIVITY OF SCREENING VOLUME SIZE TO REGIME UNCERTAINTIES

Routine conjunction risk assessment consists of predicting a close approach and analyzing the risk posed to the primary spacecraft based on repeated predictions starting at many days prior to the predicted Time of Closest Approach (TCA). During the course of a conjunction event, there may be several updates to the close approach predictions, each providing more information on the forecasted risk associated with the conjunction event. As new observations are taken on both the primary and secondary objects, the orbit determination (OD) solution for each object is updated. The estimated states and state uncertainties resulting from the OD are then propagated forward and a new TCA is determined. Typically, as the observations are updated and the propagation

time decreased, there is better orbital knowledge of the two objects at TCA and therefore more confidence in the risk assessment that results from the close approach predictions. During this refinement and update process, the close approach predictions often vary from solution to solution. It is possible that these variations may be large enough that a conjunction may be observed on one screening but not observed on a subsequent one due to the screening volume size used. An example of this prediction evolution is shown in Figure 1 for the case where the screening is done based on cross-track separation of the objects in question. Figure 1(a) depicts a time history of the cross-track miss distance with relative cross-track error bounds, (b) depicts this evolution with an a priori notion of the correct cross-track screening volume size added, (c) demonstrates how several of the event prediction updates would cause some conjunction events to fall outside this screening volume, and (d) shows how, by appropriately re-sizing the screening volume, these predictions could be captured. It is this concept that drives the screening volume sensitivity to capturing typical uncertainties in a given orbit regime.

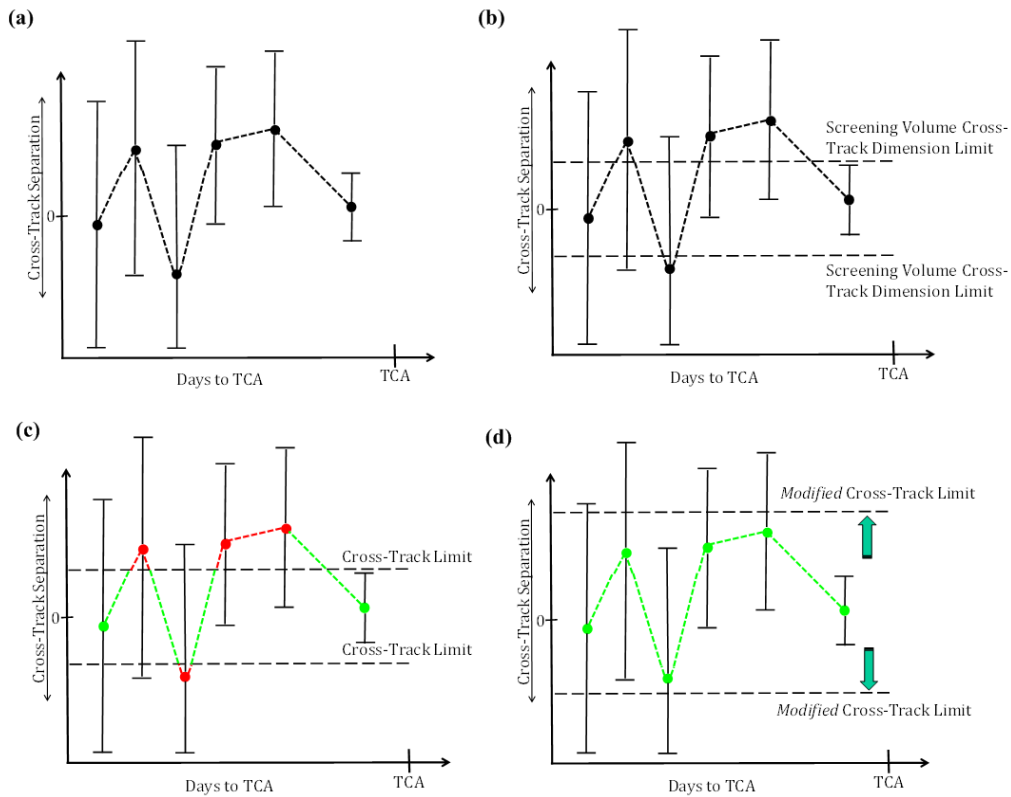


Figure 1: Notional Example of the Cross-Track Evolution of a Conjunction Event

Assuming for the moment that both objects are receiving sufficient tracking observations, this variability in predictions should be statistically bounded by the state uncertainty described by the estimated and propagated covariance matrices for the two objects. There are many object-specific factors that affect the state uncertainty of an object at any given point in time, such as the orbit, physical properties, and tracking of the object. Some factors, however, are environmental or more broad-reaching, which similarly affect all objects in the same orbital regime. It is these general effects that can be characterized by sampling historical conjunction data over the different orbital regimes, where the goal is to get a sense of the distribution of typical object uncertainties within a given orbital regime.

The combined primary-secondary uncertainty region represents the volume about an asset for which there is a possibility of the true miss vector to exist. This combined uncertainty must be calculated from the individual primary and secondary covariances provided in the close approach prediction. For this analysis, the following method was used to combine the covariance data.

State Conversions from EFR to ECI

Primary and secondary states are first converted from their respective True-Of-Date Earth Fixed Rotating (EFR) frame, as used in Orbital Conjunction Message (OCMs – the close approach prediction data type produced by the JSpOC), to a common Earth Centered Inertial (ECI) frame (J2000) at Time of Close Approach (TCA). The transformation from the EFR frame to the ECI J2000 frame is accomplished through a series of coordinate rotations. The conversion to inertial frame must account for polar motion (PM), sidereal time (ST), nutation (NUT), and precession (PREC).

The complete transformation from EFR to ECI J2000 is performed by¹

$$\bar{\mathbf{r}}_{J2000} = [\text{PREC}]^T[\text{NUT}]^T[\text{ST}]^T[\text{PM}]^T \bar{\mathbf{r}}_{EFR} \quad (1)$$

$$\bar{\mathbf{v}}_{J2000} = [\text{PREC}]^T[\text{NUT}]^T[\text{ST}]^T\{[\text{PM}]^T \bar{\mathbf{v}}_{EFR} + \bar{\boldsymbol{\omega}}_E \times \bar{\mathbf{r}}_{PEF}\}, \quad (2)$$

where $\bar{\mathbf{r}}$ and $\bar{\mathbf{v}}$ are the state position and velocity vectors, respectively, $\bar{\boldsymbol{\omega}}_E$ is the rotation rate of the Earth, and $\bar{\mathbf{r}}_{PEF} = [\text{PM}]^T \bar{\mathbf{r}}_{EFR}$.

Construction of RIC Reference Frames

Once the ECI states are known, the primary and secondary RIC frames can be constructed. Using ECI position, $\bar{\mathbf{r}}$, and velocity, $\bar{\mathbf{v}}$, define:

$$\hat{\mathbf{R}} = \frac{\bar{\mathbf{r}}}{\|\bar{\mathbf{r}}\|}, \hat{\mathbf{C}} = \frac{\bar{\mathbf{r}} \times \bar{\mathbf{v}}}{\|\bar{\mathbf{r}} \times \bar{\mathbf{v}}\|}, \hat{\mathbf{I}} = \hat{\mathbf{C}} \times \hat{\mathbf{R}}, \quad (3)$$

and form the orthogonal RIC basis, $[\hat{\mathbf{R}}, \hat{\mathbf{I}}, \hat{\mathbf{C}}]$, and denote these bases as M_p and M_s for the primary and secondary, respectively.

Combining Primary and Secondary Object Covariance

Position covariance matrices (3x3) are formed for each of the primary and secondary objects in their respective RIC frame and are denoted ${}^{RIC}\mathbf{C}_p$ and ${}^{RIC}\mathbf{C}_s$ for the primary and secondary, respectively. Then the transformation to J2K can be completed for each covariance as

$${}^{J2000}\mathbf{C}_p = [M_p]^T {}^{RIC}\mathbf{C}_p [M_p] \quad (4)$$

$${}^{J2000}\mathbf{C}_s = [M_s]^T {}^{RIC}\mathbf{C}_s [M_s] \quad (5)$$

Lastly, the primary and secondary covariances, now both in J2K, are added and rotated into the asset RIC frame, M_p :

$${}^{RIC}\mathbf{C}_{Combined} = [M_p] [{}^{J2000}\mathbf{C}_p + {}^{J2000}\mathbf{C}_s] [M_p]^T \quad (6)$$

Once the primary-secondary combined covariance is computed, statistical analysis is performed to characterize the distribution of the combined covariance in each orbital regime. The data was collected over the last five years across the defined LEO and GEO regimes. For each regime a sequence of three cumulative distribution function (CDF) plots is generated for , 1) Radial capture percentiles by *primary* propagation time, 2) In-Track capture percentiles by *primary* propagation time and 3) Cross-Track capture percentiles by *primary* propagation time. The RIC capture component values are the combined uncertainty values corresponding to historical conjunction events. In other words, the component uncertainty value corresponding to a particular percentage represents the combined uncertainty under which that percentage of events were ‘captured’. The CDF plots are presented using a logarithmic, rather than a linear, horizontal axis. This scale makes it possible to clearly view the full range of data. The plots for each regime, with the exception of the LEO #1 regime, are separated into prediction time bins of (0 – 2) days, (2 – 4) days, (4 – 6) days, and (> 6) days. The reason for binning the prediction time is due to the fact that this combined uncertainty is heavily dependent on propagation time, and that not all satellites are screened for the same time span. For example, satellites with maneuver capability may require longer lead times in order to plan and execute a collision avoidance maneuver and, hence, need to be screened further into the future. This screening span may also be a function of other constraints such as the ability to accurately propagate out a large portion of the object catalog. Figure 2 is an example of one CDF plot; this one is for the combined in-track uncertainty relative to the primary object.

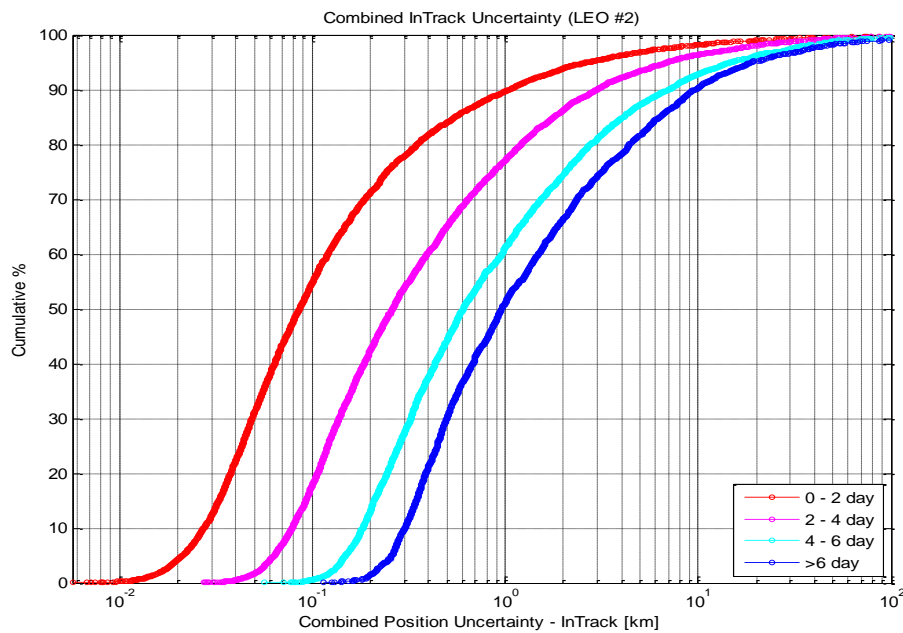


Figure 2: CDF of Primary-Secondary One-Sigma Combined Position Uncertainty for the LEO #2 Regime.

These CDF plots form the basis of one of the dimensions of the screening volume trade space: the sensitivity of screening volume size to regime uncertainty. The complete set of CDFs for the LEO and GEO regimes can be found in the Appendices.

DETERMINING SENSITIVITY OF EXPECTED EVENTS TO SCREENING VOLUME SIZE

The second sensitivity to consider in selecting a screening volume size is the number of expected conjunction events that may be observed given the selected screening volume. A simple, first order model for the relationship between screening axes and expected events (per day per asset), was determined from historical NASA / GSFC conjunction data as well to provide a truth reference for the analytically-determined estimate. The data sets used to produce this model were chosen to ensure that the number of screened assets did not change over the time span examined. For each regime, a data set of 100 random volumes were selected by producing 100 sets of 3 random numbers in [0, 1] and applying those values to the maximum radial, in-track, and cross-track screening axes for that regime. These 100 R, I, C values were then used to produce test volumes for which the number of unique conjunction events detected within that volume was determined. These event number values were then averaged over the collection time span and over the number of distinct assets composing that data set to produce an average events/asset/day value. This computation provides an average conjunction observation rate, or, the number of events per day per primary observed within that given volume.

Initial analysis of the actual events for each regime showed the radial axis to be dominant with respect to the number of observed events, largely due to the radial being the smallest axis in all cases. Additionally, for all regimes, the observed events showed a highly linear (straight line) correlation to radial screening axis size. Analysis of several methods to best fit the event/asset/day yielded similar results to the initial linear model. For these reasons, a standard form linear model was used.

$$(Events / Asset / Day) = \beta_0 r + \beta_1 i + \beta_2 c \quad (7)$$

Where r , i and c represent, respectively, the chosen radial, in-track, and cross-track screening axes, in kilometers. Application of a least squares method was used to estimate the regression coefficients, which are given for each regime in Table 2.

Table 2: Model Coefficients

| Orbital Regime | Model Coefficients | | |
|----------------|--------------------|-----------|-----------|
| | β_0 | β_1 | β_2 |
| LEO #1 | 0.3990 | 0.0026 | 0.0010 |
| LEO #2 | 0.4243 | 0.0054 | 0.0128 |
| LEO #3 | 0.3595 | 0.0075 | 0.0319 |
| LEO #4 | 0.0219 | 0.0012 | 0.0003 |
| GEO | 0.0017 | 0.0015 | 0.0001 |

In order to assess adequacy of the Event Sensitivity Model, the standard and adjusted coefficients of multiple determination (R^2) were calculated and are shown for each regime's model in Table 3. The R^2 give an indication of the variability in the model output that has been captured by the chosen regressor variables. While the R^2 calculated for each regime can be categorized² as showing a 'high correlation' of regressor variables to model output, the linear model is not ideal. However, for the purpose of this analysis, they suffice as first order predictions for each regime. It remains a future work item to redefine this model as sufficient data becomes available.

Also, a general test for significance of regression was run on each model. The test hypothesis used was as follows:

$$H_0: \beta_0 = \beta_1 = \beta_2 = 0$$

$$H_1: \beta_i \neq 0 \text{ for at least one } i$$

The test statistic, $F_0 = MS_R/MS_E$ was used, where MS_R is the regression mean square and MS_E is the residual mean square. Rejection of the null hypothesis would occur for $F_0 > F_{0.05, 3, 97}$ (= 2.60). F_0 was computed for the model of each regime and are shown in Table 3. With each model producing an F_0 greater than the rejection value the conclusion can be made that H_0 is false and that each model's dependence on *at least one* of the radial, in-track, or cross-track screening axis sizes is appropriate. Given that all axes must be specified to define a screening volume there was no reason to conclude that *any* of the axes is not relevant and further testing to refine the dependence on any of the individual axes was not pursued.

Table 3: Model Adequacy Parameters

| Orbital Regime | Adequacy Parameters | | | Mean err |
|----------------|---------------------|--------|----------------|----------|
| | F_0 | R^2 | adjusted R^2 | |
| LEO #1 | 101 | 0.7578 | 0.7528 | -0.022 |
| LEO #2 | 60 | 0.6505 | 0.6433 | -0.017 |
| LEO #3 | 55 | 0.6308 | 0.6323 | -0.016 |
| LEO #4 | 38 | 0.5400 | 0.5305 | -0.001 |
| GEO | 87 | 0.7289 | 0.7233 | -0.001 |

INTERPRETING THE SCREENING VOLUME TRADE SPACE

With the characterization of the screening volume sensitivity to event capture and the expected numbers of conjunction events observed, the trade space between these sensitivities can be fully defined. To fully determine a screening volume, one must first make a determination of the acceptable risk tolerance. The chosen screening axes may then be examined using the appropriate Event Sensitivity Model to approximately assess the workload associated with the chosen volume.

For example, if one desired to capture 90% of the events for an asset located in the LEO #2 regime being screened 7 days out; first, one must determine the appropriate 90% axes from Figure B - 1, Figure B - 2, and Figure B - 3 in Appendix B for the LEO #2 regime. The 90% capture volume from these plots has a 0.25 km Radial axis, a 10 km In-Track axis and an 11 km Cross-Track axis. Using the Event Sensitivity Model with the LEO #2 coefficients, the estimated number of Events Per Asset Per Day (EPAPD) then can be assessed as $EPAPD = 0.4243*(0.25 \text{ km}) + 0.0054*(10 \text{ km}) + 0.0128*(11 \text{ km}) = 0.3$. So, at 90% in LEO #2, one would expect to see an average of 0.3 events/day for a single asset, or about 2 events per week.

If the resulting EPAPD number exceeds what can be handled operationally, then one may choose a lower capture threshold until the trade-off between detecting all possible potential high risk conjunctions and analyst workload capacity is satisfied.

Continuing the example, if the satellite O/O had a constellation of 100 satellites, then the 0.3 EPAPD would result in an average of 30 events per day, which may exceed the system capability

to process or analyst workload to evaluate. If so, and if the O/O would be willing tolerate a 75% capture threshold, then the resulting estimate drops to an EPAPD of approximately 0.1, or 10 events per day based on the 100 satellite constellation.

THE SCREENING VOLUME SELECTION PROCESS FOR NASA LEO AND GEO ASSETS

This section is intended to walk the reader through the screening volume selection process that was performed for CARA at NASA / GSFC, using the steps outlined previously. NASA / GSFC performs routine and high interest CARA for approximately 55 Earth-orbiting missions, primarily in the LEO and GEO orbit regimes. The CARA Concept of Operations includes identification and delivery of close approach predictions by the JSpOC, conjunction risk assessment and analysis performed at NASA / GSFC, and execution of any coordinated and planned collision avoidance or mitigation strategies by mission Owner/Operators.^{3,4}

The first step of the screening volume selection process was to determine the conjunction screening span desired. For NASA, this determination is generally a function of the operability status of the primary and its ability to react to conjunction risks. Inactive primaries, of which there are none currently incorporated in the CARA process, are screened three days into the future. The three day prediction span allows adequate time for close approach trending, requesting increased tasking if needed to update tracking on the secondary object, and sufficient analysis time to characterize conjunction risk at TCA. Active missions that do not have maneuver capability but have other options for mitigating or preparing for conjunction risk, such as re-orienting to minimize apparent cross-section area, safing instruments, or staffing for emergency response and recovery, are screened five days into the future. The five-day prediction span allows for the same conjunction risk refinement as discussed for inactive missions, plus an additional two days for planning and execution of non-maneuver mitigative actions. Finally, for primaries with propulsive and maneuver capabilities, NASA uses a seven-day screening span⁵. This span allows for an additional two days for the added planning, coordination, and execution complexity for performing a conjunction mitigation maneuver. The screening spans used operationally at NASA / GSFC are summarized in Table 4.

Table 4: NASA / GSFC Screening Span by Satellite Operability

| Satellite Operability | Screening Span |
|------------------------------|-----------------------|
| Active, and Maneuverable | ≥ 7 Days |
| Active, but Non-Maneuverable | ≥ 5 Days |
| Inactive | ≥ 3 Days |

With the selection of the desired screening span, the figures in the Appendices can be consulted to determine the screening volume size. As mentioned previously, NASA currently has approximately 55 primaries included in the CARA process, most of which are in the LEO or GEO orbit regimes. The principal reason for the existing CARA process is flight safety. As a continuation of that theme, when evaluating which capture percentage to choose operationally, the NASA / GSFC desire was to capture as many potential high risk conjunctions as possible without significantly overburdening analysis resources. Prior to completion of this analysis, all LEO regimes were screened at 0.5km x 5km x 5km radial, in-track, cross-track respectively and GEO as a 15km sphere. The uncertainty capture percentages of the previous screening volumes used for CARA at NASA / GSFC are provided in Table 5.

Table 5: Previous Uncertainty Capture

| Orbital Regime | Previous Uncertainty Capture [%] | | |
|----------------|----------------------------------|----------|-------------|
| | Radial | In-Track | Cross-Track |
| LEO #1 | 77 | 29 | 28 |
| LEO #2 | 95 | 82 | 83 |
| LEO #3 | 98 | 88 | 49 |
| LEO #4 | 96 | 93 | 92 |
| GEO | 96 | 90 | 97 |

For the current CARA mission set at NASA / GSFC, a 95% uncertainty capture resulted in about 23.3 expected events per day. Compared to the previous screening volumes shown in Table 5, the 95% uncertainty capture is a marked improvement, especially in the low altitude LEO regimes. The resulting expected number of events across the entire mission set was well within system and analyst workload capacity since sufficient resources have been devoted to those endeavors.

The final screening volumes recommended for CARA operations at NASA / GSFC are provided in Table 6. Due to the small amount of data at the 7 day screening level and the large uncertainties in a number of those observations for the GEO regime, the CDFs (**Error! Reference source not found. - Error! Reference source not found.**) for GEO have significant tail contributions. Moreover, the 95% uncertainty capture resulted in in-track and cross-track screening volume dimensions that could not be used operationally. Since the EPAPD for 90% and 95% were similar for GEO, it was determined that 90% uncertainty for GEO which would still capture most events while keeping the screening volumes modest and operationally feasible. Finally, screening volumes were rounded up to the nearest kilometer (or half-kilometer in the case of radial dimensions less than one kilometer) for operational convenience.

Table 6: Final NASA LEO and GEO Screening Volume Sizes

| Orbital Regime | Uncertainty Capture | Screening Span | Screening Volume Size [km] | | | Events Per Asset Per Day |
|----------------|---------------------|----------------|----------------------------|----------|-------------|--------------------------|
| | | | Radial | In-Track | Cross-Track | |
| LEO #1 | 95 % | 3 Days | 1.5 | 69 | 145 | 0.93 |
| | | 5 Days | 1.5 | 69 | 145 | 0.93 |
| | | 7 Days | 1.5 | 69 | 145 | 0.93 |
| LEO #2 | 95 % | 3 Days | 0.5 | 7 | 7 | 0.34 |
| | | 5 Days | 0.5 | 15 | 15 | 0.48 |
| | | 7 Days | 0.75 | 20 | 22 | 0.71 |
| LEO #3 | 95 % | 3 Days | 0.5 | 5 | 3 | 0.31 |
| | | 5 Days | 0.5 | 8 | 5 | 0.40 |
| | | 7 Days | 0.5 | 11 | 9 | 0.55 |
| LEO #4 | 95 % | 3 Days | 0.5 | 3 | 4 | 0.02 |
| | | 5 Days | 0.5 | 6 | 6 | 0.02 |
| | | 7 Days | 0.5 | 8 | 10 | 0.02 |
| GEO | 90 % | 3 Days | 1.5 | 11 | 2 | 0.02 |
| | | 5 Days | 1.5 | 18 | 2 | 0.03 |
| | | 7 Days | 1.5 | 18 | 3 | 0.03 |

CONCLUSION

This analysis has presented a method for appropriately sizing screening volumes for inclusion in a conjunction risk assessment concept of operations for satellites operating in the LEO or GEO regimes. This method has considered the trade-off between the desire to capture all conjunctions that may pose a safety risk to a primary asset of concern and the ability to process and analyze those events. The paper also provides the tools and procedure for choosing those screening volumes.

For NASA, whose priority has always been with flight safety, the trade space became nearly one-dimensional as the concern was more with capturing a significant percentage of potential high risk conjunctions and less with the resulting number of events identified. Moreover, at the time the screening volumes size were being re-considered at NASA / GSFC, only the sensitivity of uncertainty capture analysis was conducted; as such, a capture threshold of 95% was chosen. This selection is preserved with additional analysis on expected events.

ACKNOWLEDGMENTS

This paper was supported by the National Aeronautics and Space Administration (NASA) / Goddard Space Flight Center (GSFC), Greenbelt, MD, under the Flight Dynamics Support Services (FDSS) contract (NNG10CP02C), Task Order 21.

REFERENCES

- ¹ Vallado, D.A., "Fundamentals of Astrodynamics and Applications", Microcosm Press, El Segundo, CA, Kluwer Academic Publishers, Dordrecht, Netherlands, 2004.
- ² Williams, Frederick and Monge, Peter, "Reasoning with Statistics: How to Read Quantitative Research", Harcourt Inc., Orlando, FL, 2001.
- ³ Narvet, S. Technical Memorandum. FDSS-21-0031. 17 September 2010.
- ⁴ Newman, L. and Duncan, M. "Establishment and Implementation of a Close Approach Evaluation and Avoidance Process for the Earth Observing Missions." AIAA-2006-6291. Conference Proceedings. *AIAA/AAS Astrodynamics Specialist Conference*. 21-24 August 2006. Keystone, CO.
- ⁵ Frigm, R., J. Levi, and D. Mantziaras, "Assessment, Planning, and Execution Considerations for Conjunction Risk Assessment and Mitigation Options." Conference Proceedings. *AIAA SpaceOps Conference*. 25-30 April 2010. Huntsville, AL.
- ⁶ Montgomery, Douglas and Elizabeth Peck. "Introduction to Linear Regression Analysis, Second Edition." New York: John Wiley & Sons, Inc., 1992.
- ⁷ Rice, John A. "Mathematical Statistics and Data Analysis." Belmont, CA: Duxbury Press, 1995.

APPENDIX A: SCREENING VOLUME TRADE SPACES FOR THE LEO #1 REGIME

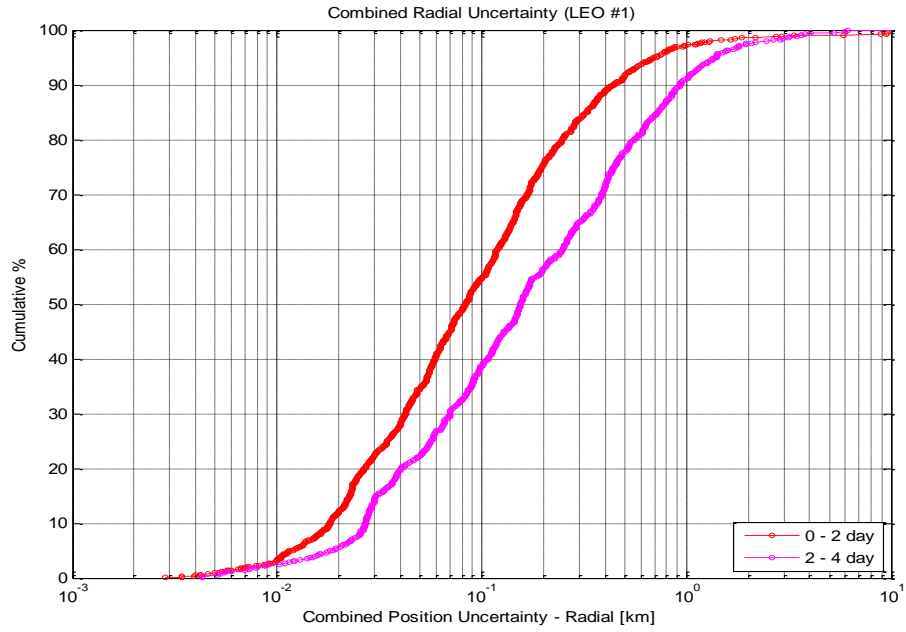


Figure A - 1: LEO #1 Radial CDF

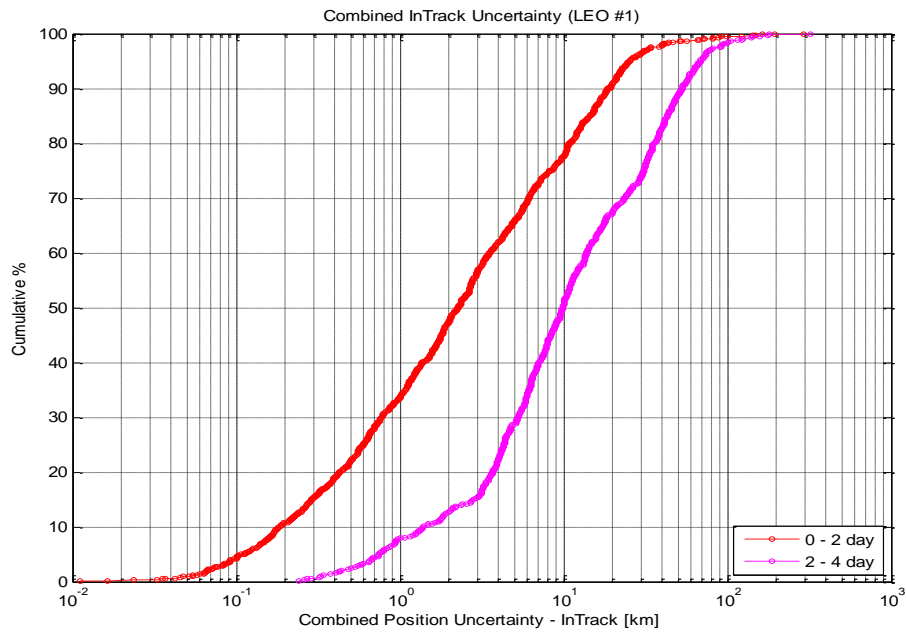


Figure A - 2: LEO #1 In-Track CDF

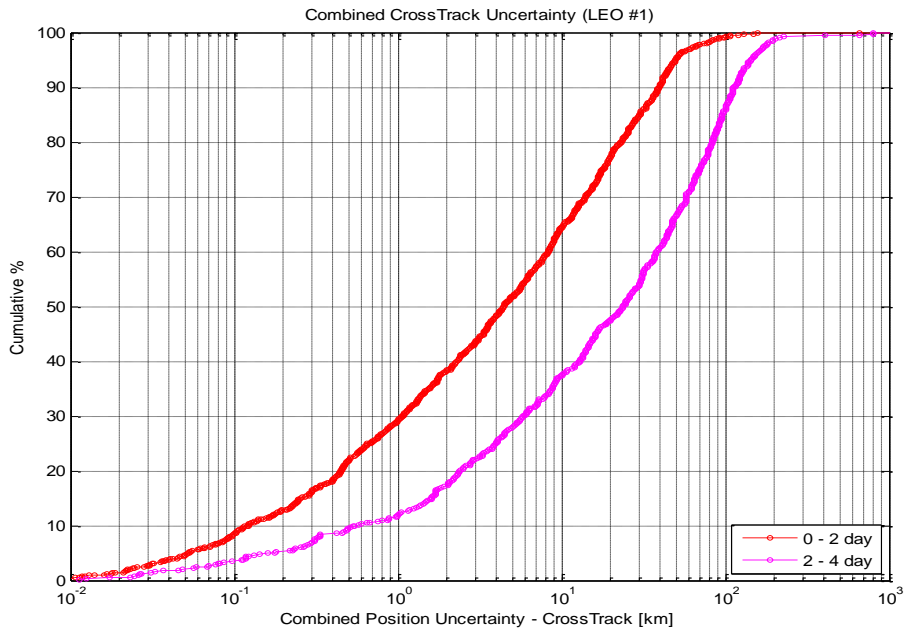


Figure A - 3: LEO #1 Cross-Track CDF

APPENDIX B: SCREENING VOLUME TRADE SPACES FOR THE LEO #2 REGIME

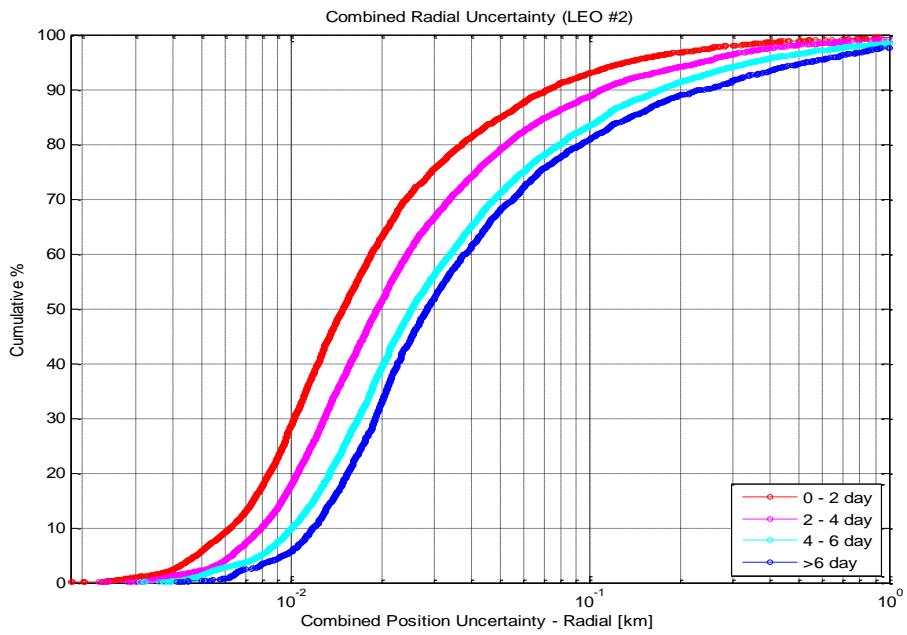


Figure B - 1: LEO #2 Radial CDF

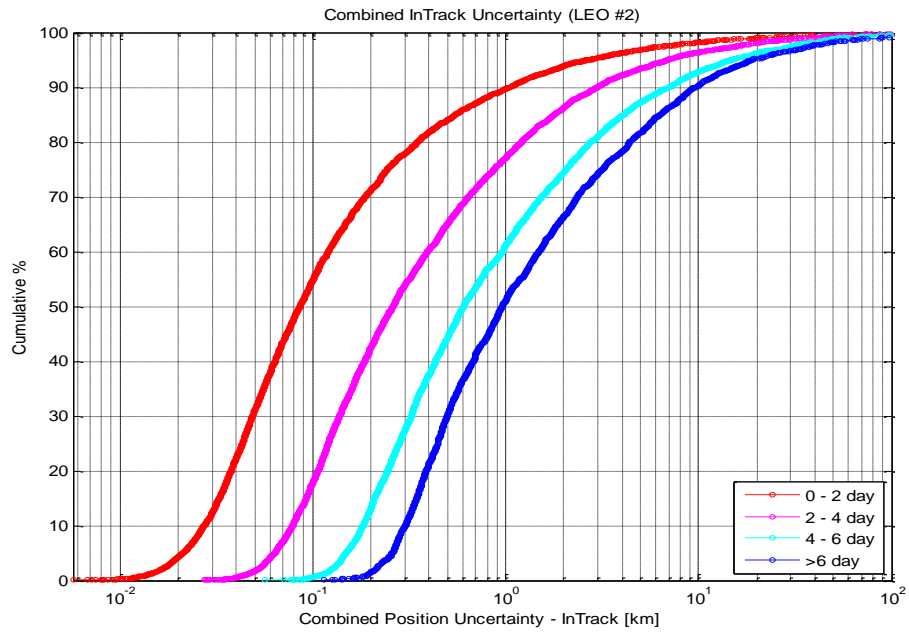


Figure B - 2: LEO #2 In-Track CDF

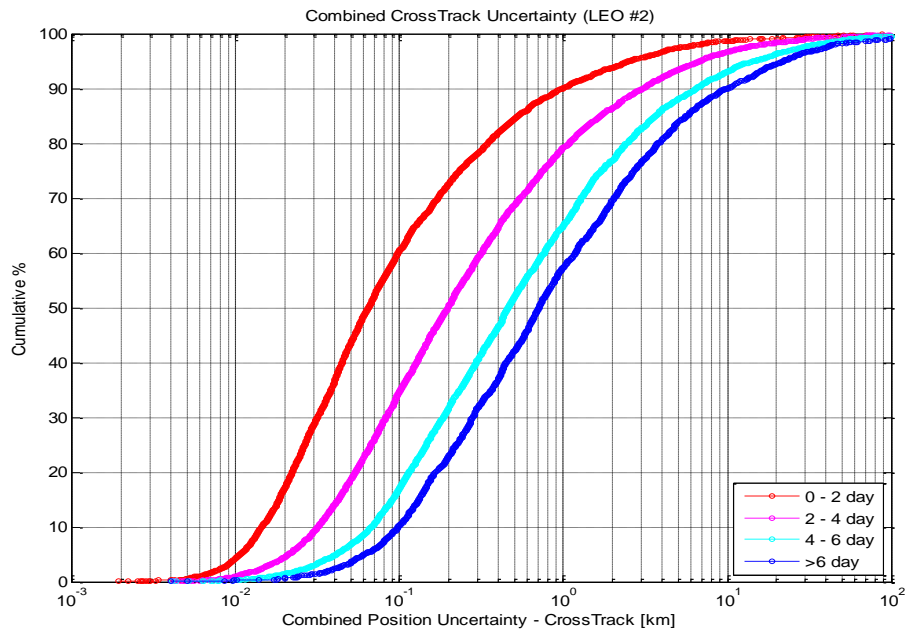


Figure B - 3: LEO #2 Cross-Track CDF

APPENDIX C: SCREENING VOLUME TRADE SPACES FOR THE LEO #3 REGIME

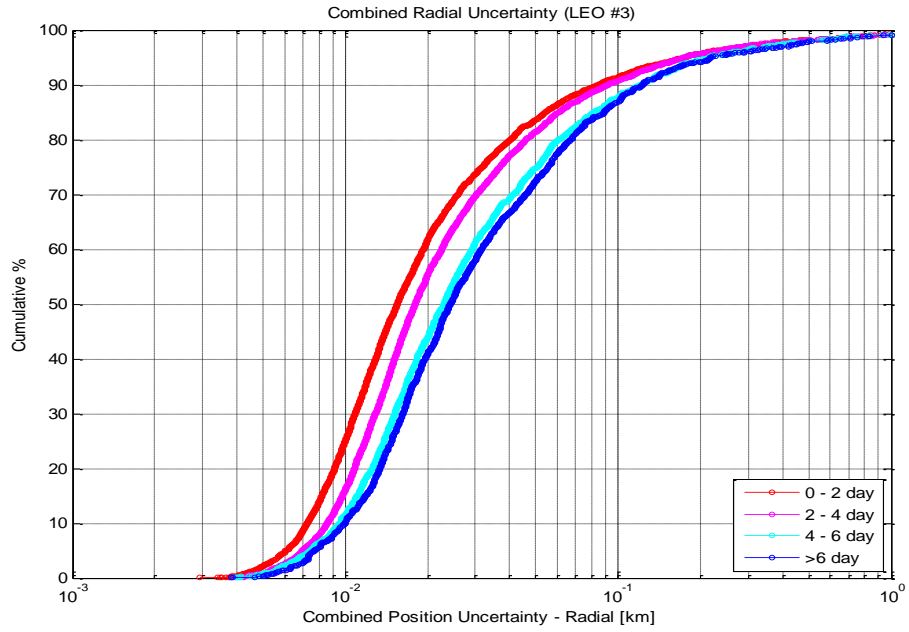


Figure C - 1: LEO #3 Radial CDF

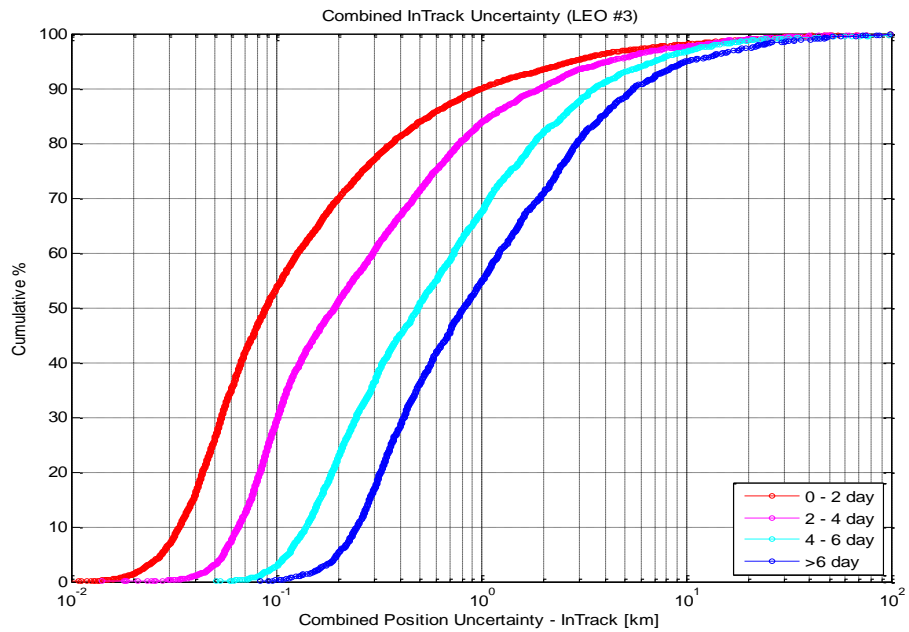


Figure C - 2: LEO #3 In-Track CDF

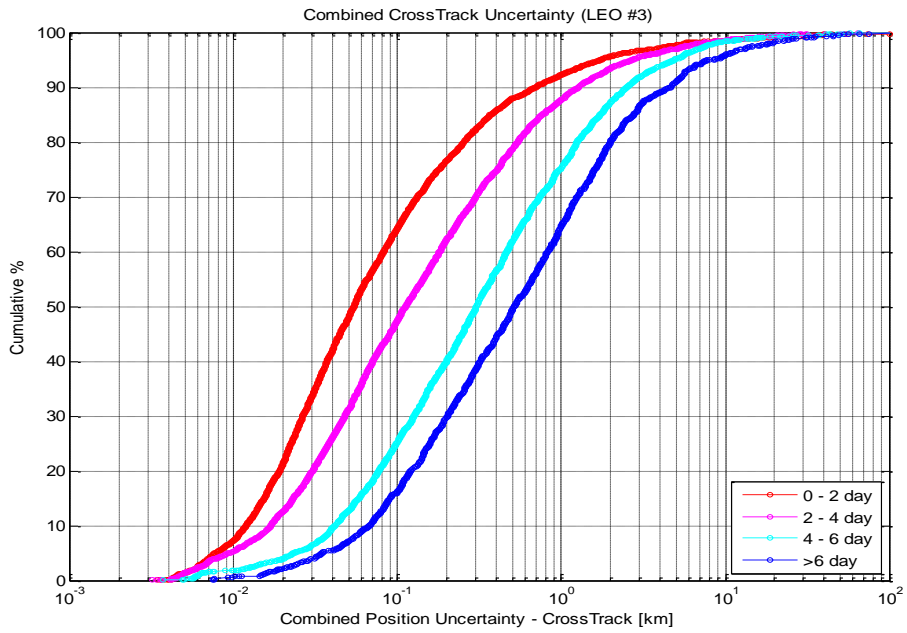


Figure C - 3: LEO #3 Cross-Track CDF

APPENDIX D: SCREENING VOLUME TRADE SPACES FOR THE LEO #4 REGIME

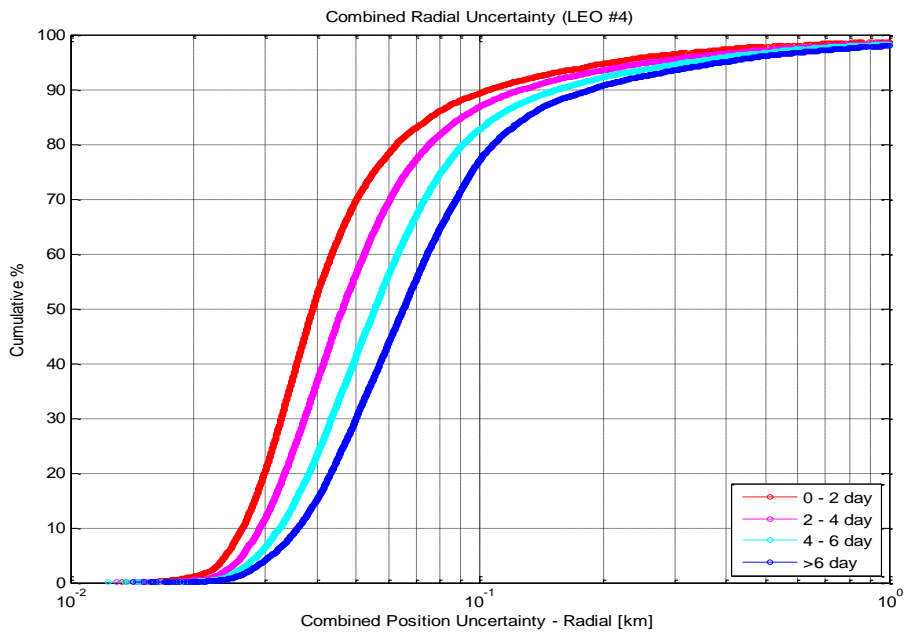


Figure D - 1: LEO #4 Radial CDF

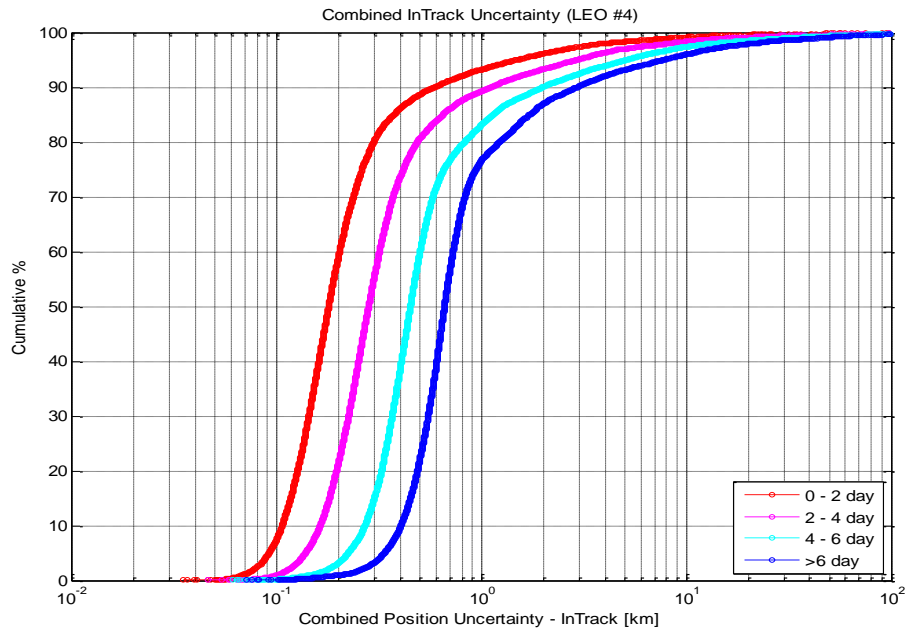


Figure D - 2: LEO #4 In-Track CDF

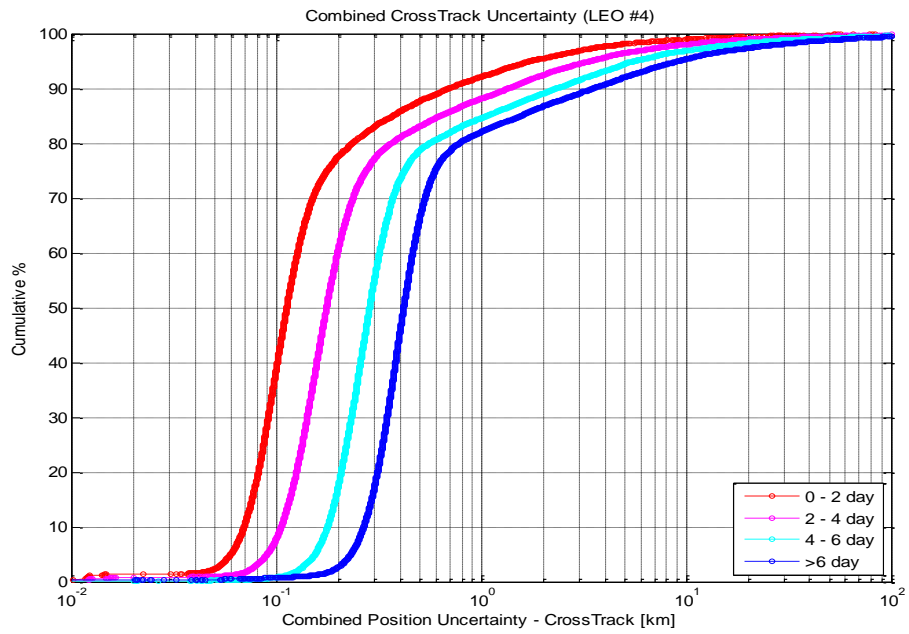


Figure D - 3: LEO #4 Cross-Track CDF

APPENDIX E: SCREENING VOLUME TRADE SPACES FOR THE GEO REGIME

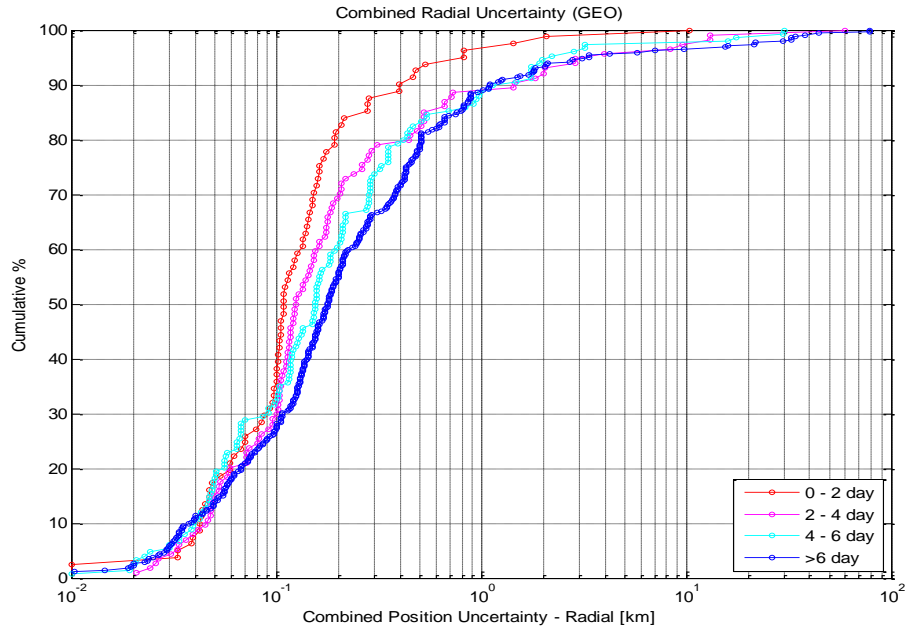


Figure E - 1: GEO Radial CDF

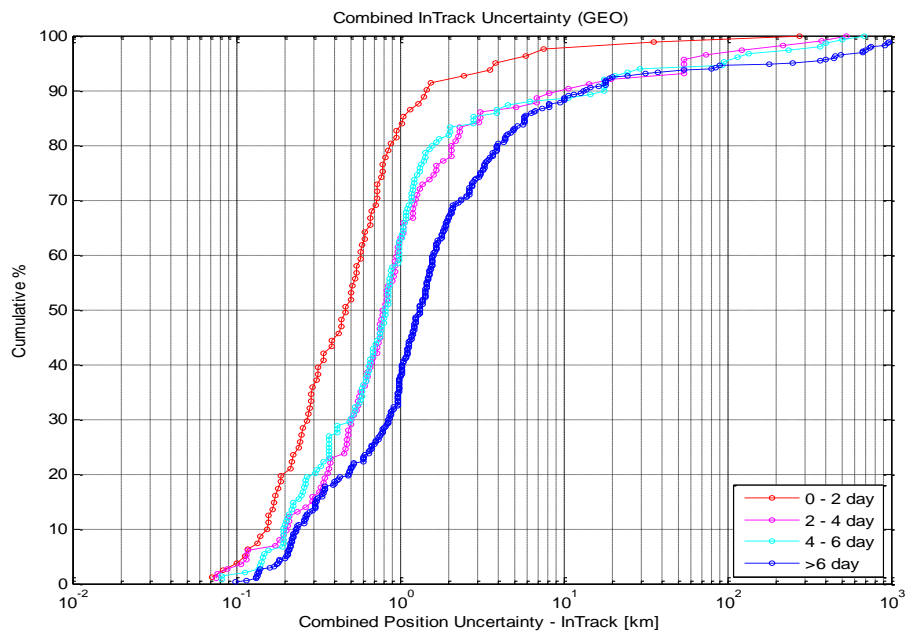


Figure E - 2: GEO In-Track CDF

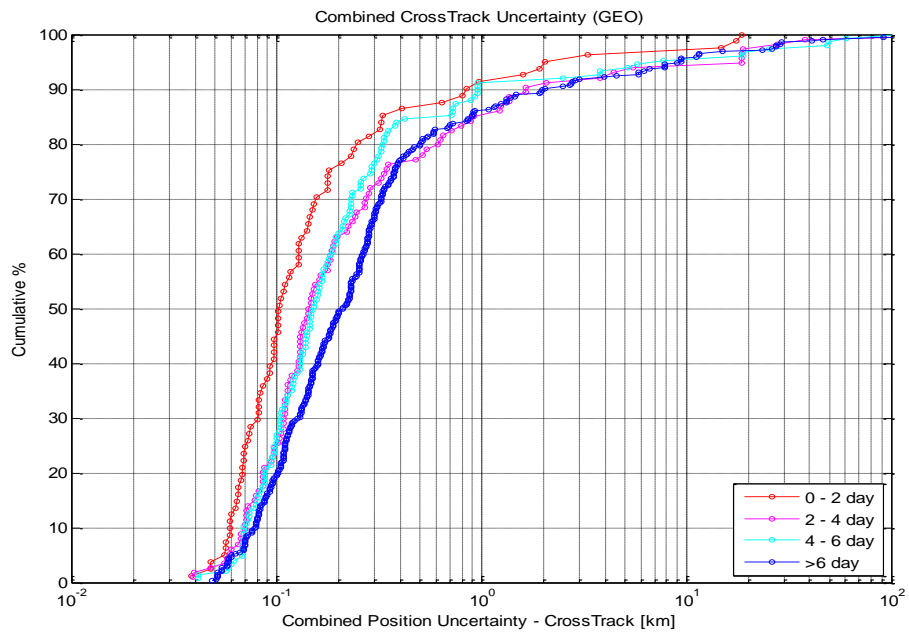


Figure E - 3: GEO Cross-Track CDF